Ultrasound-triggered disruption and self-healing of reversibly cross-linked hydrogels for drug delivery and enhanced chemotherapy

Nathaniel Huebsch[a,b,c,1,2], Cathal J. Kearney[a,b,2], Xuanhe Zhao[a,b,d,2], Jaeyun Kim[a,b,e], Christine A. Cezar[a,b], Zhigang Suo[a], and David J. Mooney[a,b,3]

[a]Harvard University School of Engineering and Applied Sciences, Cambridge, MA 02138; [b]Wyss Institute for Biologically Inspired Engineering, Cambridge, MA 02138; [c]Harvard-MIT Division of Health Sciences and Technology, Cambridge, MA 02139; [d]Soft Active Materials Laboratory, Department of Mechanical Engineering and Materials Science, Duke University, Durham, NC 27708; and [e]School of Chemical Engineering, Sungkyunkwan University, Suwon 440-746, Korea

Edited by Robert Langer, Massachusetts Institute of Technology, Cambridge, MA, and approved June 3, 2014 (received for review March 24, 2014)

Biological systems are exquisitely sensitive to the location and timing of physiologic cues and drugs. This spatiotemporal sensitivity presents opportunities for developing new therapeutic approaches. Polymer-based delivery systems are used extensively for attaining localized, sustained release of bioactive molecules. However, these devices typically are designed to achieve a constant rate of release. We hypothesized that it would be possible to create digital drug release, which could be accelerated and then switched back off, on demand, by applying ultrasound to disrupt ionically cross-linked hydrogels. We demonstrated that ultrasound does not permanently damage these materials but enables nearly digital release of small molecules, proteins, and condensed oligonucleotides. Parallel in vitro studies demonstrated that the concept of applying temporally short, high-dose "bursts" of drug exposure could be applied to enhance the toxicity of mitoxantrone toward breast cancer cells. We thus used the hydrogel system in vivo to treat xenograft tumors with mitoxantrone, and found that daily ultrasound-stimulated drug release substantially reduced tumor growth compared with sustained drug release alone. This approach of digital drug release likely will be applicable to a broad variety of polymers and bioactive molecules, and is a potentially useful tool for studying how the timing of factor delivery controls cell fate in vivo.

self-healing materials | alginate | on-demand delivery | sonophoresis

Polymer-based systems for drug delivery typically are engineered to yield a constant rate of release of bioactive compounds (1). Emergent clinical situations (e.g., pain attacks or infections) may create a need for significantly different drug doses over short periods, and in some cases, circadian drug timing increases effectiveness (2, 3). Likewise, controlled-release systems may be applied to dissect roles for specific physiologic cues or drugs during tissue development or regeneration, as these signals often are highly transient and may play opposite roles, depending on the timing of activation (4–7). Typical drug delivery systems that rely on polymer degradation and passive diffusion to control release allow precise spatial localization of cues, but not the ability to temporally control release rates at will. In contrast, on-demand release systems, such as "smart" polymers or materials activated by external stimuli [e.g., magnetic fields, radio waves, or light (8–13)] potentially offer this temporal flexibility and are beginning to be applied in the clinical setting (14). Ultrasound commonly is used in medicine and can deliver focused energy of varying magnitude and frequency with high spatiotemporal resolution (15). In particular, ultrasound has been used to trigger release from polymers by causing their degradation (16, 17). This degradation permanently changes the delivery vehicle, thus altering the baseline rate of molecular release as well as the release achieved with subsequent exposure to ultrasound. Interestingly, ultrasound also is used in a process known as sonophoresis, in which sound waves are applied to disrupt skin transiently for needle-free transdermal drug delivery (15, 18). A crucial difference between sonophoresis and ultrasound-stimulated polymer degradation is that the damage induced by cavitation during sonophoresis is only temporary, because skin has a self-healing capability that switches delivery off following removal of the ultrasound stimulus. Because self-healing causes skin to revert to its basal state following removal of the ultrasound stimulus, repeated sonophoresis yields similar doses during each pulse (15, 18). A hydrophobic coating on a drug-containing polymer disk was shown to be disrupted by ultrasound and subsequently to reform on the polymer returning release to baseline; however, a self-healing coating is susceptible to replacement by nonspecific adhesion of proteins and cells in vivo, which would result in unpredictable release kinetics (19). Thus, we sought to develop an injectable monolithic system that can hold more drug per unit volume, responds to ultrasound, and subsequently self-heals. We first demonstrated that monolithic alginate hydrogels exhibited such behavior, and that this enabled on-demand delivery of drugs, cytokines, and condensed plasmid DNA (pDNA). In vitro experiments demonstrated that human breast cancer cells were more sensitive to high-dose "pulses" of the chemotherapeutic drug mitoxantrone than they were to the

Significance

Drug-releasing polymers give clinicians the ability to deliver chemotherapy directly to tumors, sparing the rest of the body from toxic side effects. Most devices deliver a constant, unchangeable drug dose over time. However, we found that cancer cells are more sensitive to short-term, high-dose "bursts" of the chemotherapeutic mitoxantrone than to constant doses over longer periods, suggesting a benefit for implantable devices that allow external control over dose and timing. Biocompatible, injectable alginate hydrogels displayed the ability to self-heal damage induced by ultrasound pulses, enabling on-demand delivery of mitoxantrone, in vitro and in vivo, and mitoxantrone-loaded gels implanted near tumors were more effective at eliminating tumor growth when a daily pulse of ultrasound was applied.

Author contributions: N.H., C.J.K., X.Z., Z.S., and D.J.M. designed research; N.H., C.J.K., X.Z., J.K., and C.A.C. performed research; N.H., C.J.K., and X.Z. contributed new reagents/analytic tools; N.H., C.J.K., and X.Z. analyzed data; Z.S. and D.J.M. supervised research; and N.H., C.J.K., and D.J.M. wrote the paper.

The authors declare no conflict of interest.

This article is a PNAS Direct Submission.

[1]Present address: Gladstone Institute of Cardiovascular Disease, San Francisco, CA 94158.

[2]N.H., C.J.K., and X.Z. contributed equally to this work.

[3]To whom correspondence should be addressed. E-mail: mooneyd@seas.harvard.edu.

This article contains supporting information online at www.pnas.org/lookup/suppl/doi:10.1073/pnas.1405469111/-/DCSupplemental.

same drug when it was applied at a lower dose over a longer period, which motivated us to apply the drug-loaded monolithic alginate system to treat breast cancer xenografts. Treatment of xenograft breast tumors with a drug-laden gel was more effective when a daily pulse of ultrasound was applied. These findings indicate that the timing, as well as the localization of drug delivery, both influence efficacy toward chemotherapy and suggest classes of hydrogel systems that might be used to identify optimal treatment regimens and ultimately apply them clinically.

Results and Discussion

To test whether there were injectable and monolithic biomaterials that could exhibit self-healing characteristics that would allow repeated and reversible ultrasound-induced disruption (and concurrent drug release) in a manner analogous to skin sonophoresis, we first examined alginate (20), a polysaccharide that forms a hydrogel via ionic cross-linking with divalent cations (e.g., Ca^{2+}). We hypothesized that ultrasound could disrupt calcium cross-links to accelerate drug release, but the presence of Ca^{2+} in physiological fluids would allow cross-links to reform upon removal of the stimulus (Fig. 1*A*), facilitating reversible, on-demand release. On both the macroscopic and microscopic levels, substantial disruption of the structure of ionically cross-linked hydrogels was apparent after ultrasound treatment in the absence of physiologic levels of free divalent cations (Fig. 1 *B* and *C*). Interestingly, the levels of applied ultrasound power required to achieve these effects were similar to levels previously used in sonophoresis (18). In contrast, subjecting hydrogels to ultrasound treatment in the presence of free divalent cations resulted in no observable, permanent disruption of the gel structure after cessation of ultrasound, as treated gels looked identical to untreated controls (Fig. 1*D*). Mechanical properties analysis was consistent with these structural observations: the dry mass of calcium alginate hydrogels after treatment remained unchanged as long as gels were incubated in media with physiologic Ca^{2+} levels (2.6 mM; Fig. 1*E*), whereas it dropped substantially when gels were treated with ultrasound while maintained in Ca^{2+}-depleted saline. This finding was verified further by measurements of elastic modulus, a more sensitive metric of relative cross-link density and mechanical integrity than dry mass (Fig. 1*F*). Consistent with the hypothesis that cross-links reform upon removal of the ultrasound in a manner dependent on the presence of free calcium in the surrounding fluid, calcium alginate gels bathed in media with supraphysiological Ca^{2+} levels became stiffer upon repeated ultrasound treatment (Fig. 1*F*).

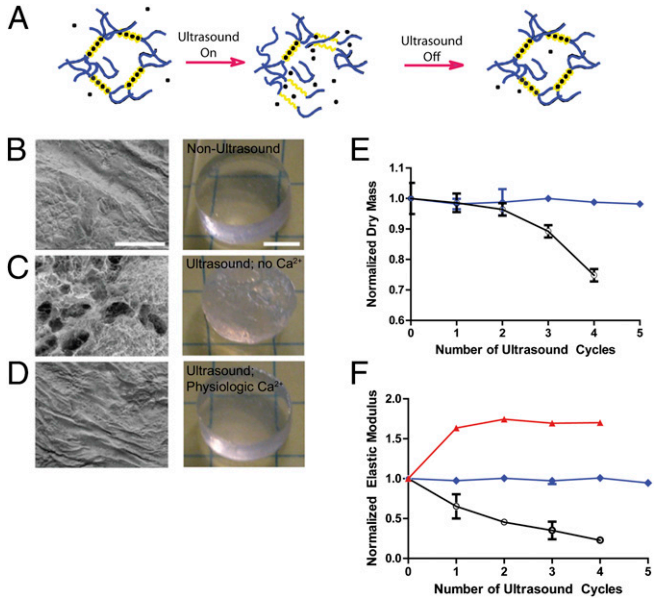

Fig. 1. Ultrasound-induced disruption and self-healing of ionically cross-linked hydrogels. (*A*) Schematic of the proposed ability of ultrasound to induce transient disruption of hydrogels cross-linked by calcium, followed by reformation of cross-links by calcium within physiologic fluids, resulting in gel healing. Calcium (●) binds selectively to guluronic acid chains (yellow) of alginate polymers. (*B–D*). Scanning electron micrographs (SEMs) of the microstructure (*Left*) and photographs of the gross structure (*Right*) of (*B*) calcium alginate hydrogels before ultrasound, (*C*) calcium alginate hydrogels after treatment with ultrasound in medium without divalent cations, and (*D*) calcium alginate hydrogels after treatment with ultrasound in medium with physiologic levels of Ca^{2+}. (*E* and *F*) Normalized dry mass (*E*) and normalized elastic modulus (*F*) of alginate hydrogels exposed to ultrasound while bathing in medium without divalent cations (○), media with 2.6 mM Ca^{2+} (blue ◆), or media with a supraphysiologic concentration (13.3 mM) of Ca^{2+} (red ▲). Error bars: SD, $n = 4$. Scale bars (*B–D*): SEM, 200 μm; photographs, 5 mm.

The possibility of using reversible, ultrasound-triggered disruption of ionic cross-links to induce bursts of drug release was investigated next. Mitoxantrone, an anthracycline commonly used to treat breast cancer, is a charged molecule that forms an ionic complex with alginate (21) and thus exhibited a low baseline level of release from alginate gels in the absence of ultrasound (Fig. 2 *A* and *C*). One of the drawbacks of mitoxantrone clinically is its off-target toxicity, which may be minimized in this system by local delivery of the chemotherapeutic. To monitor ultrasound-induced release, drug-loaded, preswollen hydrogels were moved to fresh media and pulsed with ultrasound. Immediately following treatment, gels were moved to a new container to monitor release without stimulus. To account for any release induced by mechanical handling (22), gels not exposed to ultrasound also were moved to new media at the same time intervals. Handling alone had a minor, albeit detectable, effect on the release rate of mitoxantrone in the absence of ultrasound (Fig. 2 *A* and *C*). Pulsatile ultrasound application triggered mitoxantrone release, leading to visible depletion of the drug (blue) from hydrogels and accumulation within the media surrounding the gels (Fig. 2 *B* and *C*). To test ultrasound-mediated release in vivo, we switched to a shear-thinning gel formulation that could be delivered precisely and noninvasively (23). This gel formulation exhibited similar, ultrasound-triggered drug release, again without undergoing degradation (as judged by the reversibility of release kinetics when ultrasound was removed) in vitro (Fig. S1), compared with the original formulation. In vivo, even a single pulse of ultrasound substantially increased drug release into the s.c. space in nude mice (Fig. 2 *D* and *E*).

The broader utility of ultrasound-stimulated gel disruption toward macromolecular delivery next was tested on condensed oligonucleotides and cytokines. Positively charged condensed pDNA and the extracellular matrix-binding cytokine stromal cell-derived factor 1α (SDF-1α) both interact strongly with alginate (13, 24), minimizing their baseline levels of release from non-degrading hydrogels. Like mitoxantrone, both these macromolecules were released in a pulsatile manner via ultrasound treatment (Fig. 2 *F* and *G*), leading to stepwise accumulation in the medium surrounding the gels. VEGF-165, another cytokine that interacts noncovalently with alginate (22), although not with the same strength as SDF-1α, also was released in an on-demand manner with ultrasound (Fig. S2). Further mechanistic studies were consistent with the assumption that ultrasound causes on-demand drug release via transient gel disruption and that the primary means of release is through the gel surface (*SI Materials and Methods* and Figs. S3–S5).

To determine whether reversible, ultrasound-triggered release is possible with other types of hydrogels, we investigated the release of naproxen (a negatively charged nonsteroidal anti-inflammatory drug) from ionic hydrogels formed by cross-linking the polycationic polymer chitosan with tripolyphosphate (TPP).

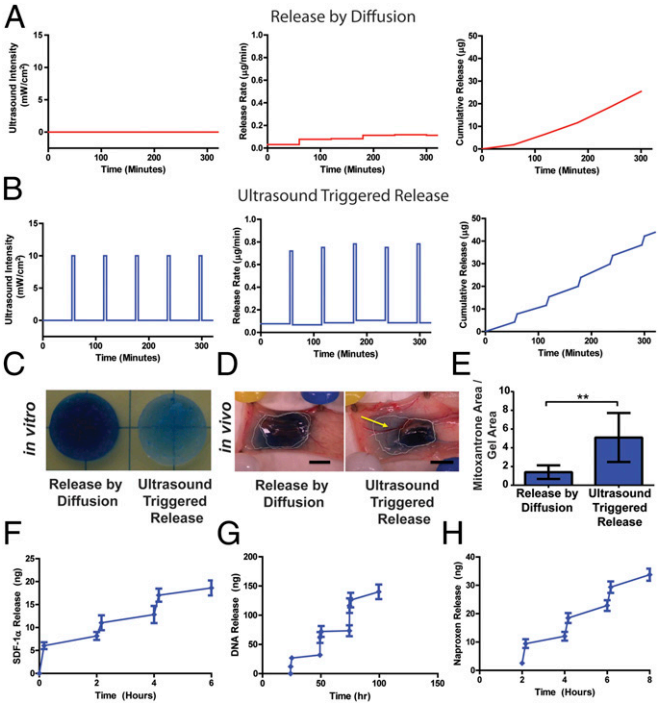

Fig. 2. Ultrasound-mediated on-demand release from ionically cross-linked hydrogels. (*A* and *B*) Quantitative analysis of mitoxantrone release via diffusion (*A*) or ultrasound treatment (*B*; 5 min, applied once every hour). Data indicate ultrasound intensity (*Left*), mitoxantrone release rate (*Center*), and cumulative mitoxantrone release (*Right*). (*C*) Representative images of residual mitoxantrone (blue) contained in alginate hydrogels after they were treated with ultrasound once per hour over 10 h (*Right*) or not treated with ultrasound (*Left*). (*D*) Representative images of residual mitoxantrone contained in alginate hydrogels, and mitoxantrone released from gels and subsequently deposited into host tissues, after hydrogels were transplanted into Nu/J mice and treated once with ultrasound for 2.5 min (*Right*) or left untreated (*Left*) over a 24-h period. (*E*) Quantitative analysis of the extent of in vivo mitoxantrone release, determined by the total surface area of s.c. tissue displaying visible staining with the drug (blue) normalized to the area of the transplanted gels. (*F*) Cumulative delivery of SDF-1α from hydrogels that were treated with ultrasound for 10 min once every 2 h. (*G*) Cumulative delivery of pDNA condensed with poly(ethylene imine) from hydrogels that were treated with ultrasound for 10 min once every day. (*H*) Cumulative delivery of naproxen from TPP–chitosan hydrogels treated with ultrasound for 10 minutes once every 2 h. Error bars: SD, $n = 3$–4. *$P < 0.05$, *t* test.

Ultrasound treatment significantly enhanced naproxen release from these materials (Fig. 2*H*). Accordingly, these data suggest that a wide variety of bioactive molecules might be released in a pulsatile fashion, given the appropriately selected drug–gel pairing. With the appropriate choice of drugs and/or carrier molecules, one may be able to integrate ultrasound-mediated drug delivery into complex devices that release multiple compounds over different time frames (14).

As cancer cells specifically have been shown to exhibit dynamic responses to drug treatment (3, 4), we hypothesized that intermittent, higher pulses of drug dose might enhance the effects of chemotherapeutic drugs such as mitoxantrone. To test this hypothesis, we first analyzed the effects of controlling the timing of dose profiles on mitoxantrone-treated cancer cells in vitro. Two human breast cancer lines (MDA-MB-231 and MCF7) were treated with two different dose profiles of drug: (*i*) an intermediate, constant dose or (*ii*) a combination of short duration, high concentration of drug with sustained exposure to a lower baseline dose. Drug concentrations were altered via media exchange to prevent confounding of the study results by exposing cells to ultrasound or to drugs released from gels via ultrasound, and with every media change, all samples were washed thoroughly with PBS and fresh media was added to avoid any confounding effects of residual drug (from previous dosings) or media exchange on cell viability. The integrated value of drug dose over time (e.g., total drug exposure) to which cells were exposed was maintained constant. Interestingly, the combination of temporally short exposure to a burst of drug with a low baseline dose appeared to be much more effective than sustained exposure to mitoxantrone in reducing cancer cell viability (Fig. 3 *A*–*C*). Additional studies indicated that the total drug exposure also significantly contributes to the effects of mitoxantrone (Fig. S6). These results are consistent with previous work indicating that the dynamics of drug exposure have substantial effects on cell-level responses (4, 5), highlighting the importance of studying cell response to drug dynamics and the necessity for robust systems that facilitate these delivery modes in vitro and in vivo.

We then analyzed how the dynamics of mitoxantrone exposure affected viability in these cells. MDA-MB-231 cells were used in these studies, as they represent a more metastatic population than MCF7 breast cancer cells. The enhanced ability of a pulse of mitoxantrone to diminish cell viability was consistent across several dosing profiles (Fig. 3*D*). Further, increasing the time of burst exposure while diminishing the concentration during burst (to maintain the same level of integrated drug exposure) diminished the effect of mitoxantrone, whereas using an even shorter burst time with a higher dose enhanced its effects (Fig. 3*D*).

Having established the potential therapeutic utility of combining short bursts of concentrated drug release with a baseline, lower dose of drug in vitro and identifying a set of biomaterials that would allow such profiles to be delivered in vivo, we investigated the effects of ultrasound-mediated mitoxantrone delivery on treatment of xenograft human breast tumors (MDA-MB-231) in nude mice. First, short-term studies were performed to identify effects of ultrasound-mediated drug delivery on tumor growth and apoptosis. TUNEL staining of tumors after 8 d of treatment revealed that implanting mitoxantrone-laden alginate matrices led to significant apoptosis in the xenografts, regardless of whether a daily dose of ultrasound was applied to induce burst release (Fig. 4 *A* and *B*). In contrast, systemic drug delivery of the equivalent amount of drug delivered via bolus tail vein injection did not lead to substantial apoptosis. This finding is consistent with literature reports of the poor ability of systemically delivered mitoxantrone to reach xenograft tumors [<5% of systemic dose typically found at xenograft hindlimb tumor site (25)]. Interestingly, daily local drug injections, or a bolus drug injection combined with daily ultrasound, yielded little to no improvement in xenograft apoptosis over tail vein injection. Although these results do not rule out the possibility that ultrasound might enhance tissue permeability, thereby increasing drug potency, they strongly suggest that a locally deployed drug depot is required to maintain a baseline concentration of bioactive drug. Consistent with this assumption, measurements of relative tumor size revealed that both a daily local injection of drug and the combination of basal delivery from a hydrogel combined with a daily ultrasound pulse led to a reduction in tumor size, but only the combined regimen yielded tumors that were statistically different in size than tumors from mice subjected to a systemic (tail vein) dose (Fig. 4*C*). Combined with the finding that drug-laden gels, with or without ultrasound pulsing, yielded significant levels of xenograft apoptosis, this suggests that the levels of mitoxantrone to which tumors are exposed are sufficient for eliminating tumors, but that a basal level of apoptosis is reached earlier in tumors in which drug-laden gels are pulsed with ultrasound, which translates into a substantial reduction in tumor mass. Thus, these data suggest that combining a local, basal release with intermittent

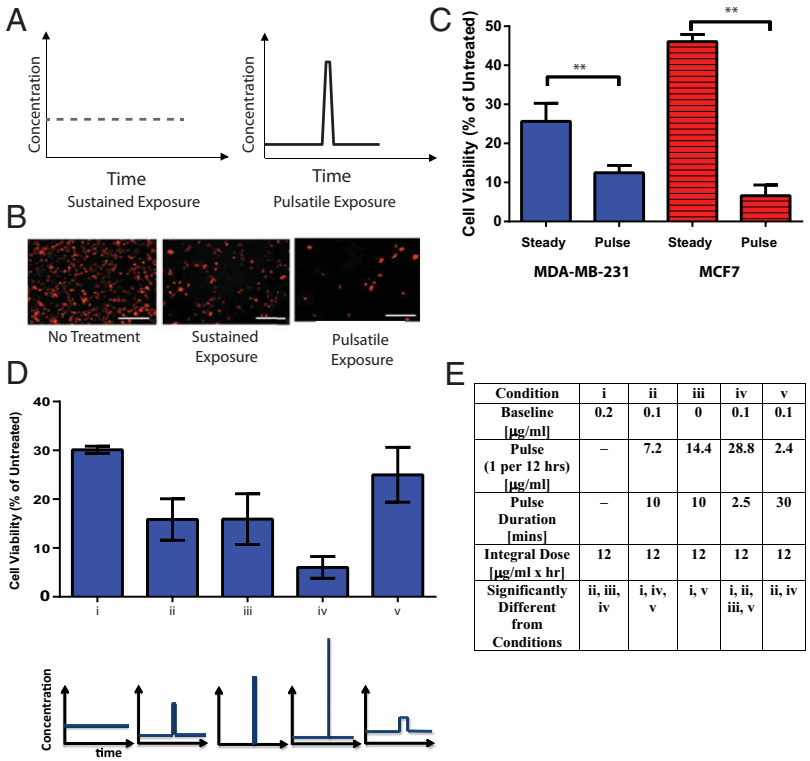

E

Condition	i	ii	iii	iv	v
Baseline [μg/ml]	0.2	0.1	0	0.1	0.1
Pulse (1 per 12 hrs) [μg/ml]	–	7.2	14.4	28.8	2.4
Pulse Duration [mins]	–	10	10	2.5	30
Integral Dose [μg/ml x hr]	12	12	12	12	12
Significantly Different from Conditions	ii, iii, iv	i, iv, v	i, v	i, ii, iii, v	ii, iv

Fig. 3. Dynamics of mitoxantrone exposure affects drug effects on viability of human breast cancer cells in vitro. (*A*) Schematics depicting constant drug concentration, representative of the dose that would be expected with standard drug-delivering biomaterials (*Left*), or a lower baseline dose, interspersed with a high dose presented in a pulsatile fashion (*Right*), representative of the dose expected with on-demand release. Note that the integrated dose is the same. (*B*) Representative fluorescence micrographs of mCherry-labeled MDA-MB-231 breast cancer cells exposed to a sustained mitoxantrone dose (*Center*) or a lower baseline drug dose interspersed with a periodic high dose, applied for 10 min once every 12 h (*Left*). (*C*) Quantitative analysis of cell viability in MDA-MB-231 (blue) and MCF7 (red) breast cancer cell lines treated with sustained or pulsatile exposure to mitoxantrone. The cycle was performed once every 12 h and repeated five times, and the total drug exposure was constant at 12 $\mu g \cdot mL^{-1} \cdot h^{-1}$ in both conditions. (*D*) Quantitative analysis of MDA-MB-231 viability after 60 h of various mitoxantrone dosing regimens. (*E*) Table detailing the dosing regimens used for *D*. Error bars: SD, $n = 4$ (**$P < 0.05$, two-tailed *t*-test), $n = 3$–9. Scale bars (*B*): 200 μm.

pulses of drug enhances treatment of tumors throughout the course of therapy.

Based on the results of our short-term studies, subsequent long-term studies on tumor growth and host survival were performed using locally deployed alginate gels. Tumors within mice receiving no therapy grew rapidly, and these animals succumbed to the effects of tumors within 100 d. Treatment with mitoxantrone-eluting gels alone decreased tumor growth rate and improved survival, as expected, with the time to 50% animal mortality increasing from 100 to 120 d (Fig. 4 *D* and *E*). Strikingly, the combination of low-level sustained release with a daily concentrated pulse of mitoxantrone delivered via ultrasound reduced the growth rate of xenograft tumors compared with treatment with mitoxantrone-laden gels alone (Fig. 4*D*). Importantly, this treatment improved survival of mice bearing these tumors after all treatments had stopped, with the time to 50% animal mortality nearly doubling from the value of 100 d for mice receiving no therapy to 180 d (Fig. 4*E*). Kaplan–Meir analysis revealed a statistically significant survival improvement in mice treated with either drug-laden gels or drug-laden gels exposed to a daily pulse of ultrasound, compared with mice receiving no therapy. Although survival did not improve significantly when daily ultrasound pulses were applied on top of the drug-laden gels, tumors were significantly smaller in this treatment group (compared with tumors in mice receiving only drug-laden gels) from days 10 through 70 of treatment (with the exception of days 24–31 and days 59–63). Notably, the drug payload within ultrasound-treated gels is depleted faster than the drug within gels loaded with drug but not exposed to this stimulus (Fig. S7)—hence, mitoxantrone-laden gels not treated with ultrasound continued to release drug for a longer period; thus, the net amount of drug delivered to tumors over the course of this study was the same between these conditions. These results suggest that although localized mitoxantrone delivery is therapeutic, its effectiveness—and likely the effectiveness of other existing drugs—may be improved with optimal spatial as well as temporal delivery.

At the end of the 6-mo study period, surviving mice were euthanized and the masses of remaining tumors were analyzed. Tumors within surviving mice that had received a combination of ultrasound and mitoxantrone-laden hydrogels had not grown substantially since the start of treatment (Fig. 4*F*) and had a net mass of 63 ± 45 mg. In contrast, among tumors retrieved from surviving mice that had received mitoxantrone-laden hydrogels but not ultrasound, only one of the remaining tumors weighed less than 100 mg, whereas the other weighed nearly 1 g, or the approximate mass of tumors explanted from drug-treated mice that succumbed to tumors earlier in the study (1,100 ± 800 mg).

Although the current studies demonstrate the potential of ultrasound-stimulated drug release to enhance chemotherapy, it is noted that further testing mimicking the exact application is required before its clinical adoption. The ultrasound intensities are within those used by other authors for ultrasound-stimulated drug release and were demonstrated to be safe in animal testing (17, 18). More sophisticated ultrasound devices that focus the signal on the gel would allow deeper implantation of the gel and mitigate any potential side effects. Such devices also would allow

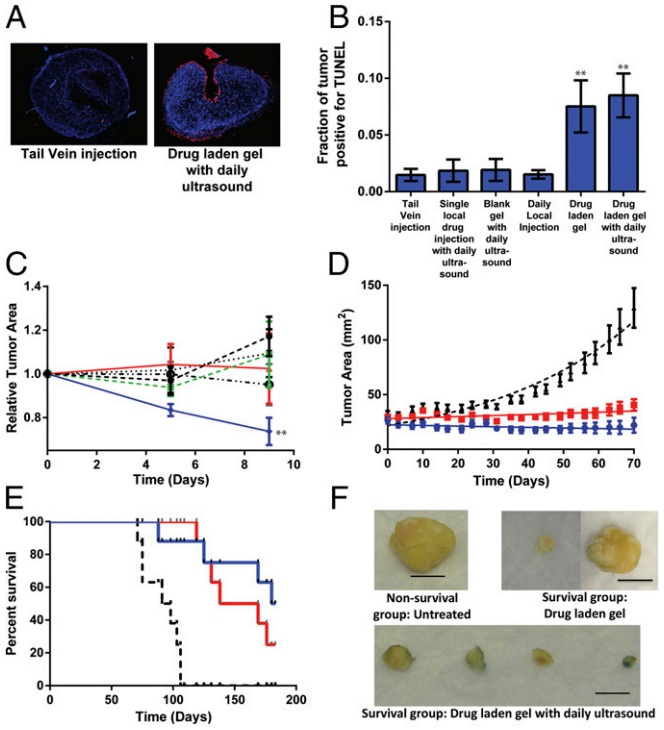

Fig. 4. Ultrasound-mediated local drug delivery diminishes xenograft tumor growth. (*A*–*C*) Short-term studies of xenograft tumor growth and apoptosis when treated with ultrasound-triggered mitoxantrone. (*A* and *B*) Representative images (*A*) and quantitative analysis (*B*) of TUNEL-stained tumor sections from mice bearing tumors that were treated via systemic tail vein mitoxantrone bolus or with various local delivery regimes. (*C*) Normalized area of tumors treated via systemic mitoxantrone dose (single tail vein injection of the maximum tolerated dose, 82.5 μg; black ●); local injection of the maximum tolerated dose of mitoxantrone followed by daily pulses of ultrasound (green ■); locally deployed mitoxantrone-laden alginate gel (red ▲); daily pulse of ultrasound on a blank, locally deployed alginate gel (black ▼); daily local mitoxantrone injections (black ○); or a locally deployed, mitoxantrone-laden alginate gel subjected to daily pulses of ultrasound (blue ◆). Ultrasound was applied for 2.5 min. (*D*) Growth curves for human MDA-MB-231 breast cancer xenografts in Nu/J mice. Tumors were left untreated (black curve), exposed to a standard alginate gel loaded with mitoxantrone but not ultrasound (red curve), or treated with a combination of mitoxantrone-laden hydrogels and daily ultrasound (blue curve). Tumor size differences were statistically significant in the mitoxantrone-laden gels treated with daily ultrasound vs. the untreated control from day 7 until the end of the study, and vs. the mitoxantrone-laden hydrogel from day 7 until the end of the study with the exception of days 24–31 and days 59–63. (*E*) Survival curves for mice left untreated between 70 and 180 d following tumor implantation, after receiving no treatment (black curve), treatment with a mitoxantrone-laden gel but no ultrasound (red curve), or treatment with a combination of mitoxantrone-laden gel and daily ultrasound treatment (blue curve). Kaplan–Meier analysis revealed a statistically significant survival improvement in mice treated with either drug-laden gels or with drug-laden gels exposed to a daily pulse of ultrasound, compared with mice receiving no therapy. (*F*) Images of tumors explanted at the end of the study from nonsurviving mice (no treatment) and surviving mice (drug alone and drug-laden gel treated with daily ultrasound pulse). Error bars: SEM, $n = 5$–8 (short-term tumor growth studies and TUNEL staining; $^{**}P < 0.05$ compared with tail vein injection, Holm–Bonferroni test) or $n = 10$ (long-term tumor growth studies and survival studies). Scale bar (*F*): 1 cm.

xenograft tumors to be implanted directly into the mammary gland (i.e., orthotopic models) or would enable the use of mouse models in which breast tumors develop spontaneously (26, 27). In the present study, the mammary gland was avoided because the distance between the skin and lungs in the mouse is very short compared with the distance between these tissues in humans.

Alginate gels previously were used clinically and have been tested by numerous investigators in animal models, supporting the eventual application of this material in clinical use. As demonstrated here, other types of hydrogels (or appropriate carrier molecules) may be necessary for pulsatile delivery of molecules with substantially different charge or structure compared with mitoxantrone (e.g., naproxen). Applications that may benefit from intermittent high pulsing (e.g., cancer therapy, pain management) or from applications that require release of a drug or factor at specific time points (e.g., in tissue engineering) might benefit greatly from the described system.

Together, the results presented here indicate that self-healing, ionically cross-linked polymers subject to ultrasonic irradiation can trigger on-demand drug delivery in vivo and augment the effects of sustained, baseline release. We also demonstrate a potential therapeutic application of this technology. Combining mitoxantrone with other drugs or macromolecules [e.g., siRNAs (28)] likely will further enhance the therapeutic efficacy of this system. We expect this technology to be applied to many polymers that form ionically or physically cross-linked gels, enabling externally triggered release of a wide variety of factors, including small molecules, proteins, nucleic acids, and nanoparticles (29–31). Beyond clinical applications, this technique also may be useful in fundamental studies of how the delivery profile or timing of application of bioactive agents modulates tissue development, pathology, and regeneration.

Materials and Methods

Alginate Hydrogels and Analysis of Self-Healing. Medical grade, high guluronic acid-content, high M_r alginate (MVG) was purchased from FMC Biopolymers. Alginates were dialyzed against water, filtered (0.22-μm mesh), freeze dried, and resuspended into Dulbecco's PBS (dPBS; Invitrogen). For drug, protein, and pDNA release studies, the alginate polymers first were combined with the molecule of interest to facilitate noncovalent interactions. Next, alginate was cross-linked with calcium sulfate ($CaSO_4$; Sigma) to a final concentration of 50 mM Ca^{2+} and 20 mg/mL MVG within gels, and a biopsy punch was used to obtain gels of a defined size and shape. Hydrogels were equilibrated overnight in serum free DMEM without phenol red (Invitrogen). Next, gels were transferred to 15-mL tubes filled with dPBS with an additional 0–13.3 mM Ca^{2+}. Gels were subjected to ultrasound treatment (9.6 mW/cm^2, 5-min pulses, once per hour). The power and time of ultrasound application were chosen based upon measurements of the temperature of media subjected to ultrasound, and within the range used here, temperature change did not exceed controls (controls were kept at 37 °C; ultrasound was done at room temperature, and the media temperature remained <32 °C), allowing any change in molecular diffusion coefficients or hydrogel degradation via heat to be ruled out of our analysis. To assess gross structural changes, gels that had been subjected to four ultrasound treatments were photographed and immediately flash frozen in liquid nitrogen. After freeze drying, ultrastructure was assessed using a Zeiss EVO scanning electron microscope at the Harvard Center for Nanoscale Systems. To detect cross-linking changes, gels were subjected to a set number of ultrasound treatments, and elastic modulus was measured using an Intron 3342 mechanical testing apparatus. Immediately after modulus testing, gels were flash frozen and lyophilized to obtain their dry masses.

In Vitro Hydrogel Self-Healing and Release Studies. Drug-, protein-, or pDNA-laden alginate gels were cast. The final concentration of each bioactive agent within gels was as follows: mitoxantrone, 850 μg/mL of gel; SDF-1α (Peprotech), 20 μg/mL of gel; pDNA (gWiz GFP plasmid DNA, Aldevron), 100 μg/mL of gel. Ultrasound was applied at 9.6 mW/cm^2 for 5 min at intervals of 1 h (mitoxantrone), 2 h (SDF-1α), or 24 h (pDNA). Release was measured colorimetrically (mitoxantrone; 650 nm), by ELISA (SDF-1α), or by PicoGreen assay (pDNA).

In Vivo Hydrogel Release Study. For in vivo studies, an injectable formulation of alginate was used, as described in the text. Briefly, low M_r MVG was prepared by irradiating medical grade MVG at 5 Mrad with a cobalt source (23). A binary formulation of 20 mg/mL low M_r MVG with 0.5 mg/mL unmodified MVG was mixed with mitoxantrone (850 μg/mL of gel), then cross-linked with 4% wt/vol $CaSO_4$ (1.22 M). In vitro studies were performed to ensure that these gels exhibited on-demand release in response to ultrasound

as described for the unary MVG gels above (Fig. S1). For in vivo release analysis, gels (100 μL vol) were injected adjacent to tumors with a 23-gauge needle. One day after hydrogel injection, a subset of these gels was exposed to ultrasound for 2.5 min with a Sonics Vibra-Cell VCX130 sonicator (13-mm–diameter horn, 120 mW/cm^2). The ultrasound transducer was coupled to the underlying alginate hydrogel by applying a thick layer of Aquasonic 100 Medical Ultrasound Transmission Gel (Parker Laboratories). The extent of drug release was analyzed in a blinded fashion by assessing the area of s.c. tissue stained with mitoxantrone (blue) and normalizing to the area of the hydrogel.

Xenograft Tumor Studies. All animal experiments were performed according to established animal protocols. Tumors were created by injecting 10^6 MDA-MB-231 cells (American Type Cell Culture) combined with Matrigel (BD Biosciences) to a total volume of 200 μL (100 μL PBS and 100 μL Matrigel) into the hindlimbs of 8-wk-old Nu/J mice (The Jackson Laboratory). Following 3 wk of tumor inoculation, the mice used for the study were normalized for tumor size by selecting mice with tumors of area between 20 and 45 mm^2; estimated cross-sectional areas were calculated as the area of a circle with the average of the shortest and longest tumor dimensions. These mice were distributed randomly in seven groups and treated as described in Table S1.

Injectable alginate formulations, as described above for in vivo release studies, were used and injected with a 23-gauge needle into adjacent tumors. A drug dosage of 85 μg per animal was chosen because it yields a systemic dose of ∼3.1 mg/kg, within the dosage range previously shown to reduce xenograft tumor burden in nude mice treated i.v. with mitoxantrone (22, 32). Ultrasound treatments were applied for 2.5 min/d with a Sonics Vibra-Cell VCX130 sonicator (2.5 min/d, 13-mm–diameter horn, 120 mW/cm^2) once every 24 h. As in the initial in vivo release studies, the ultrasound transducer was coupled to the injected hydrogel by using a thick layer of Aquasonic 100 Medical Ultrasound Transmission Gel applied to the skin of the mice. Mice were killed on day 8 (24 h after final ultrasound treatment/injection). Tissue was formalin fixed and paraffin embedded. Next, tissue samples were encoded so they could be sectioned and analyzed in a blinded manner. Histological sections (5 μm) were taken through the middle of the tumor, and TUNEL staining was performed by using a cell death kit (Roche) at the Histology Core at the Gladstone Institute (San Francisco). For analysis of TUNEL staining, low-resolution images of the entire tumor section were taken of the TUNEL stain and DAPI counterstain using the 2.5× objective on a Biorevo BZ-9000 imaging station (Keyence). The percentage of tumor labeling positive with DAPI then was analyzed (MATLAB; MathWorks).

For the longer study, tumors were generated as above. Thirty mice with tumors ranging between 20 and 45 mm^2 in estimated area were assigned randomly to three groups: no treatment, mitoxantrone-laden gel only, or mitoxantrone-laden gel with daily ultrasound. The gel, drug, and ultrasound conditions also were identical to those above. For both the mitoxantrone-plus-ultrasound and mitoxantrone-only conditions, a new drug-laden gel was injected adjacent the tumor every 2 wk. Beginning 70 d after treatment initiation, all therapeutic treatments were stopped to assess mouse survival. Throughout the study, tumor area was measured twice per week with digital calipers, and animals were euthanized for humane reasons in consultation with the Harvard Institutional Animal Care and Use Committee, based on the following criteria: tumor >20 mm in one direction, tumor >17 mm in two dimensions, tumor >17 mm in one dimension and mouse looking cachectic, and tumor ulcerated through skin and nonhealing open wound present. Mice that died of unrelated causes were not included in the survival analysis.

ACKNOWLEDGMENTS. We thank Lewis Hahn for advice regarding pDNA delivery, as well as Ratmir Derda, Akiko Mammato, and Donald Ingber for providing the mCherry-labeled MDA-MB-231 cells. We thank Caroline Miller (Gladstone Histology Core) for performing sectioning and TUNEL staining. This work was supported by the Materials Research Science and Engineering Center at Harvard University, a California Institute of Medicine Fellowship (N.H.), and the National Institutes of Health/National Institute of Dental and Craniofacial Research (Grant R01 DE019917). X.Z. acknowledges startup funds from the Pratt School of Engineering at Duke University. J.K. acknowledges the National Research Foundation (NRF) Grant 2010-0027955 funded by the Korea government [the Ministry of Science, ICT and Future Planning (MSIP)].

1. Cao Y, Langer R (2010) Optimizing the delivery of cancer drugs that block angiogenesis. *Sci Trans Med* 2:15ps3.
2. Mormont MC, Levi F (2003) Cancer chronotherapy: Principles, applications, and perspectives. *Cancer* 97(1):155–169.
3. Peppas NA, Leobandung W (2004) Stimuli-sensitive hydrogels: Ideal carriers for chronobiology and chronotherapy. *J Biomater Sci Polym Ed* 15(2):125–144.
4. Cohen AA, et al. (2008) Dynamic proteomics of individual cancer cells in response to a drug. *Science* 322(5907):1511–1516.
5. Janes KA, et al. (2005) A systems model of signaling identifies a molecular basis set for cytokine-induced apoptosis. *Science* 310(5754):1646–1653.
6. Tay S, et al. (2010) Single-cell NF-kappaB dynamics reveal digital activation and analogue information processing. *Nature* 466(7303):267–271.
7. Ueno S, et al. (2007) Biphasic role for Wnt/beta-catenin signaling in cardiac specification in zebrafish and embryonic stem cells. *Proc Natl Acad Sci USA* 104(23): 9685–9690.
8. Huebsch N, Mooney DJ (2009) Inspiration and application in the evolution of biomaterials. *Nature* 462(7272):426–432.
9. Kearney CJ, Mooney DJ (2013) Macroscale delivery systems for molecular and cellular payloads. *Nat Mater* 12(11):1004–1017.
10. Park J-H, et al. (2010) Cooperative nanoparticles for tumor detection and photothermally triggered drug delivery. *Adv Mater* 22(8):880–885.
11. Park TG, Hoffman AS (1992) Synthesis and characterization of pH- and/or temperature-sensitive hydrogels. *J Appl Polym Sci* 46:659–671.
12. Stanley SA, et al. (2012) Radio-wave heating of iron oxide nanoparticles can regulate plasma glucose in mice. *Science* 336(6081):604–608.
13. Zhao X, et al. (2011) Active scaffolds for on-demand drug and cell delivery. *Proc Natl Acad Sci USA* 108(1):67–72.
14. Farra R, et al. (2012) First-in-human testing of a wirelessly controlled drug delivery microchip. *Sci Trans Med* 4:122ra21.
15. Mitragotri S (2005) Healing sound: The use of ultrasound in drug delivery and other therapeutic applications. *Nat Rev Drug Discov* 4(3):255–260.
16. Epstein-Barash H, et al. (2010) A microcomposite hydrogel for repeated on-demand ultrasound-triggered drug delivery. *Biomaterials* 31(19):5208–5217.
17. Kost J, Leong K, Langer R (1989) Ultrasound-enhanced polymer degradation and release of incorporated substances. *Proc Natl Acad Sci USA* 86(20):7663–7666.
18. Mitragotri S, Blankschtein D, Langer R (1995) Ultrasound-mediated transdermal protein delivery. *Science* 269(5225):850–853.
19. Kwok CS, Mourad PD, Crum LA, Ratner BD (2001) Self-assembled molecular structures as ultrasonically-responsive barrier membranes for pulsatile drug delivery. *J Biomed Mater Res* 57(2):151–164.
20. Augst AD, Kong HJ, Mooney DJ (2006) Alginate hydrogels as biomaterials. *Macromol Biosci* 6(8):623–633.
21. Bouhadir KH, et al. (2001) Degradation of partially oxidized alginate and its potential application for tissue engineering. *Biotechnol Prog* 17(5):945–950.
22. Lee KY, Peters MC, Anderson KW, Mooney DJ (2000) Controlled growth factor release from synthetic extracellular matrices. *Nature* 408(6815):998–1000.
23. Kong H, Lee K, Mooney D (2002) Decoupling the dependence of rheological/mechanical properties of hydrogels from solids concentration. *Polymer* 43:6239–6246.
24. Kong HJ, Kim ES, Huang Y-C, Mooney DJ (2008) Design of biodegradable hydrogel for the local and sustained delivery of angiogenic plasmid DNA. *Pharm Res* 25(5): 1230–1238.
25. Inoue K, Fujimoto S, Ogawa M (1983) Antitumor efficacy of seventeen anticancer drugs in human breast cancer xenograft (MX-1) transplanted in nude mice. *Cancer Chemother Pharmacol* 10(3):182–186.
26. Muller WJ, et al. (1996) Synergistic interaction of the Neu proto-oncogene product and transforming growth factor alpha in the mammary epithelium of transgenic mice. *Mol Cell Biol* 16(10):5726–5736.
27. Guy CT, et al. (1992) Expression of the neu protooncogene in the mammary epithelium of transgenic mice induces metastatic disease. *Proc Natl Acad Sci USA* 89(22): 10578–10582.
28. Goldberg MS, et al. (2011) Nanoparticle-mediated delivery of siRNA targeting Parp1 extends survival of mice bearing tumors derived from Brca1-deficient ovarian cancer cells. *Proc Natl Acad Sci USA* 108(2):745–750.
29. Zangi L, et al. (2013) Modified mRNA directs the fate of heart progenitor cells and induces vascular regeneration after myocardial infarction. *Nat Biotechnol* 31(10): 898–907.
30. Stephan MT, Moon JJ, Um SH, Bershteyn A, Irvine DJ (2010) Therapeutic cell engineering with surface-conjugated synthetic nanoparticles. *Nat Med* 16(9):1035–1041.
31. Jin DK, et al. (2006) Cytokine-mediated deployment of SDF-1 induces revascularization through recruitment of CXCR4+ hemangiocytes. *Nat Med* 12(5):557–567.
32. Rentsch KM, Horber DH, Schwendener RA, Wunderli-Allenspach H, Hänseler E (1997) Comparative pharmacokinetic and cytotoxic analysis of three different formulations of mitoxantrone in mice. *Br J Cancer* 75(7):986–992.